

# SEARCHES FOR THE NEUTRAL MSSM HIGGS BOSONS IN $e^+e^-$ COLLIDERS\*\*\*

J. ROSIEK

Institute of Theoretical Physics  
Warsaw University  
Hoża 69, 00-681 Warszawa

*(Received November 18, 1996)*

We present the techniques of the calculations of the 1-loop radiative corrections to the neutral MSSM Higgs boson masses and production cross sections in the on-shell renormalization scheme. We discuss possible applications to the analysis of experimental results from LEP1 and the expected physics potential of LEP2 and the NLC.

PACS numbers: 1260. Fr, 12.60. Jr

## 1. Introduction

The search for Higgs particles is one of the most challenging problems of experimental particle physics. Particular attention is given to the search for the Higgs bosons with properties predicted by the Minimal Supersymmetric Standard Model (MSSM). Numerous results of searches for Higgs bosons in the framework of the MSSM are reported from the LEP1 experiments [1]. The next phase of the LEP programme, LEP2, has been started reaching the energy of collisions  $\sqrt{s} > 2m_W$  [2]. The physics potential of the  $e^+e^-$  Next Linear Collider, NLC, running at energies,  $\sqrt{s} \geq 500$  GeV, is intensively discussed [3].

A realistic analysis of the phenomenology of the MSSM Higgs sector has to include radiative corrections [4–11]. Several approaches have been developed to compute radiative corrections to the tree-level approximation:

- the Effective Potential Approach (EPA) [5],
- the Renormalization Group Equations (RGE) approach [6, 7], and

---

\* Presented at the XXXVI Cracow School of Theoretical Physics, Zakopane, Poland, June 1–11, 1996.

\*\* Supported in part by the Alexander von Humboldt Stiftung and by the Polish Committee for Scientific Research.

- the Full 1-loop Diagrammatic Calculations (FDC) in the on-shell renormalization scheme [8–10].

We concentrate on the last method (FDC), which provides a systematic renormalization programme for the Higgs sector in the MSSM and is useful in several ways. First, FDC provides a “reference frame” for the other two methods which use certain approximations. It takes into account the virtual effects of all possible MSSM particles and includes contributions which have yet been neglected in the EPA, such as gauge sector contributions, momentum-dependent effects in Green’s functions, and genuine 1-loop corrections to 3- and 4-point functions [8, 9]. Thus, the accuracy of different methods in various regions of the parameter space is now well checked.

Previous interpretations in the MSSM of searches for Higgs bosons, which are performed by the LEP experiments [1], are based on common assumptions:

1. Radiative corrections to the MSSM Higgs boson masses, production and decay rates are considered in the EPA approximation, in its most simplified version. Only the leading part of the contribution arising from the top quark and from its supersymmetric scalar partner, stop, is considered.
2. The MSSM parameter space is strongly constrained by neglecting the dependence on most of the SUSY particle masses and couplings. In the most simplified version of the EPA, only one free SUSY parameter,  $m_{\tilde{t}}$  is considered.

We improve the interpretations of existing experimental results and perspectives of future searches for the neutral MSSM Higgs bosons. First, we interpret existing LEP1 data and simulations of detector efficiencies expected for LEP2 and the NLC using more accurate theoretical calculations of the production and decay rates of  $h^0$ ,  $H^0$  and  $A^0$  in the FDC approach, and then we compare the results with the EPA predictions. Second, we study the effect of using a larger set of parameters describing the MSSM, taking into account the existing experimental constraints on the SUSY parameters. We discuss three main aspects of the neutral MSSM Higgs boson searches: implications of the existing experimental data from LEP1<sup>1</sup>, perspectives of the searches at LEP2, and at the NLC.

## 2. Method of calculations

In this Section we define our renormalization scheme for the Higgs sector of the MSSM. In general we follow the notation and conventions of Ref. [14],

---

<sup>1</sup> The results presented here are based on the published measurements from the L3 collaboration [12]

where the full lagrangian and the complete set of Feynman rules for the MSSM is given. The Higgs potential has the well known form:

$$V_0 = m_1^2 \bar{H}_1 H_1 + m_2^2 \bar{H}_2 H_2 - m_{12}^2 (\varepsilon_{ab} H_1^a H_2^b + c.c.) \\ + \frac{1}{8} (g_1^2 + g_2^2) (\bar{H}_1 H_1 - \bar{H}_2 H_2)^2 + \frac{1}{2} g_2^2 |\bar{H}_1 H_2|^2. \quad (1)$$

The renormalization constants are defined as follows:

$$m_i^2 \rightarrow Z_{Hi}^{-1} (m_i^2 + \delta m_i^2), \quad m_{12}^2 \rightarrow Z_{H1}^{-1/2} Z_{H2}^{-1/2} (m_{12}^2 + \delta m_{12}^2),$$

$$v_i \rightarrow Z_{Hi}^{1/2} (v_i - \delta v_i), \quad g_1 \rightarrow Z_1 Z_B^{-3/2} g_1, \quad g_2 \rightarrow Z_2 Z_W^{-3/2} g_2,$$

$$H_i \rightarrow Z_{Hi}^{1/2} H_i, \quad B_\mu \rightarrow Z_B^{1/2} B_\mu, \quad W_\mu \rightarrow Z_W^{1/2} W_\mu. \quad (2)$$

With the fields and parameters renormalized as indicated above, we introduce a gauge fixing term (in a generalized  $R_\xi$  gauge) expressed in terms of the renormalized quantities. We choose to work in the gauge “infinitesimally” different from the ’t Hooft–Feynman gauge. Therefore we set the  $R_\xi$  gauge parameters as

$$\xi_{1,2}^{B,W} \rightarrow 1 + \delta \xi_{1,2}^{B,W} \quad (3)$$

and use  $\delta \xi_i^{B,W}$  as finite counterterms.

The counterterms defined above can be used to renormalize the gauge and Higgs boson sectors of the MSSM. Their finite parts must be fixed by choosing appropriate renormalization conditions. Below we specify our “on-shell” renormalization scheme. The quantities with a hat (which are finite) are obtained from the divergent quantities (without a hat) by adding the counterterms.

1. Gauge bosons sector. We write the 1–PI two point functions of the massive gauge boson and photon propagators as

$$i \left( g^{\mu\nu} - \frac{k^\mu k^\nu}{k^2} \right) \Pi^T(k^2) + i \frac{k^\mu k^\nu}{k^2} \Pi^L(k^2) \\ i \left( g^{\mu\nu} k^2 - k^\mu k^\nu \right) \Pi'_\gamma(k^2) \quad (4)$$

and we impose the following renormalization conditions

$$\hat{\Pi}'_\gamma(k^2 = 0) = 0 \quad \mathcal{Re} \hat{\Pi}_W^T(k^2 = M_W^2) = 0 \\ \mathcal{Re} \hat{\Pi}_{\gamma Z}^T(k^2 = 0) = 0 \quad \mathcal{Re} \hat{\Pi}_Z^T(k^2 = M_Z^2) = 0. \quad (5)$$

Thus, the tree level masses of the  $W^\pm$  and  $Z^0$  bosons are the physical ones, the on-shell photon has no mixing to  $Z^0$  and the residuum of the photon propagator equals to unity [15]. The finite counterterms  $\delta\xi_1^{B,W}$  are used to locate poles of the longitudinal parts of the gauge boson propagators at  $M_W^2$ ,  $M_Z^2$  and 0, respectively.

2. Tadpoles. In order to make contact with the effective potential approach of Ref. [5] (which uses Landau gauge) we want to work with the fields  $H^0$  and  $h^0$  which have vanishing vacuum expectation values order by order in perturbation theory. We therefore require that the sum of the tree and loop tadpoles vanishes. We fix  $\delta v_i$  (in the dimensional reduction regularization scheme) by the formula:

$$\delta v_i = \frac{1}{4(4\pi)^2} (3g_2^2 + g_1^2) v_i \left( \frac{2}{d-4} + \gamma - \log 4\pi \right) \quad (6)$$

and cancel the remaining parts of the tadpoles by the counterterms  $\delta m_1^2$  and  $\delta m_2^2$ .

3. Pseudoscalar sector. Because the mass of the  $A^0$  is usually chosen to parameterize the Higgs sector of the model, we require that the on-shell  $A^0$  does not mix with the  $Z^0$ . We write the corresponding mixed propagator as<sup>2</sup>

$$- p^\mu \Sigma_{ZP}^i(p^2) \quad i = 1, 2 \quad (7)$$

and demand

$$\text{Re } \hat{\Sigma}_{ZP}^1(M_A^2) = 0. \quad (8)$$

The finite “counterterms”  $\delta\xi_{1,2}^{\gamma Z}$  again can be used to cancel the  $\gamma - G^0$  mixing at  $p^2 = 0$ . To determine  $\delta m_{12}^2$  we require:

$$\text{Re } \hat{\Sigma}_{PP}^{11}(M_A^2) = 0. \quad (9)$$

In addition we can arrange for

$$\text{Re } \hat{\Sigma}_{PP}^{22}(M_Z^2) = 0, \quad \text{Re } \hat{\Sigma}_{+-}^{22}(M_W^2) = 0 \quad (10)$$

in order to determine the three independent constants  $\delta\xi_2^B$ ,  $\delta\xi_2^{W3}$  and  $\delta\xi_2^W$ .

---

<sup>2</sup> This is a compact version of the standard notation:  $\Sigma_{ZP}^1 \equiv \Sigma_{Z^0 A^0}$ ,  $\Sigma_{PP}^{22} \equiv \Sigma_{G^0 G^0}$ ,  $\Sigma_{SS}^{12} \equiv \Sigma_{h^0 H^0}$  etc.

4. We perform the renormalization of the fermion sector in the same way as it is usually performed in the Standard Model [15], *i.e.* we require, that  $e = g_1 g_2 / \sqrt{g_1^2 + g_2^2}$  is equal to the electric charge as measured in the Thompson limit, that is  $e^2/4\pi = 1/137.036$ .

In the MSSM the corrections to the Higgs boson masses are expected to be large. Therefore we determine the masses as the exact poles of the scalar Higgs boson  $2 \times 2$  matrix propagator:

$$\mathcal{R}e \left[ \left( p^2 - m_{H_1^0}^2 - \hat{\Sigma}_{SS}^{11}(p^2) \right) \left( p^2 - m_{H_2^0}^2 - \hat{\Sigma}_{SS}^{22}(p^2) \right) - \left( \hat{\Sigma}_{SS}^{12}(p^2) \right)^2 \right] = 0. \quad (11)$$

Such definition of the physical Higgs masses means that a summation has been performed over all 1-P reducible self-energy diagrams with one-loop segments.

### 3. Parameter space of the MSSM

The most general version of the MSSM Lagrangian contains a large number of free parameters. Most of the parameters describing SUSY particles (referred to as SUSY parameters) have small impact on the Higgs sector. Using numerical simulations, we identified which parameters are important for the Higgs boson phenomenology. These parameters have been varied independently:

- $(m_h, m_A)$  or  $(m_H, m_A)$  – the investigated Higgs boson mass combinations.
- $m_{sq}$  – the common mass parameter for all squarks. The assumption of the same mass parameters for the three squark generations has a small effect. Results depend mostly on the stop mass parameter and only weakly on the masses of other sfermions.
- $m_g$  – the gaugino mass. We assumed the commonly used GUT relation for the SU(2) and U(1) gaugino masses:  $m_{U(1)} = \frac{5}{3} \tan^2 \theta_W m_{SU(2)}$ ,  $m_{SU(2)} = m_g$ . This assumption also has a little impact on results.
- $\mu$  – the mixing parameter of the Higgs doublets in the superpotential.
- $A$  – the mixing parameter in the sfermion sector. As for  $m_{sq}$  only one universal parameter is considered for all generations. The mixing is proportional to  $A m_{sq}$ .

Throughout our paper, the top quark mass is fixed to  $m_t = 175$  GeV [16]. In order to study the effect of the variation of the SUSY parameters described above we scan them in the ranges given in Table I.

TABLE I

Ranges of SUSY parameters used for independent variation in the study of the MSSM neutral Higgs boson searches.

Parameter	$m_{sq}$ (GeV)	$m_g$ (GeV)	$\mu$ (GeV)	$A$
Range	200—1000	200—1000	−500—500	−1—+1

The parameters shown in Table I are the input parameters for the calculations of the physical sfermion, chargino, and neutralino masses. Some parameter combinations can be unphysical (*e.g.* negative squark masses) or experimentally excluded. Such cases are removed by imposing the following constraints: stop and chargino are required to be heavier than  $m_Z/2$ , and the neutralino to be heavy (or weakly coupled) in agreement with the bound on contributions to the  $Z^0$  width beyond the MSM:  $\Delta\Gamma_Z^{\max} < 31$  MeV [17]. An additional constraint is applied on  $\tan\beta$ , defined as the ratio of the vacuum expectation values of the Higgs doublets. In our approach  $\tan\beta$  is a function of  $m_h$ ,  $m_A$  and the SUSY parameters listed in Table I. Tree-level experimental bounds on  $\tan\beta$  are assumed to hold approximately, and its value is constrained to  $0.5 \leq \tan\beta \leq 50$ . The lower bound is based on [18]. The variation of the upper bound has no significant effect on the results. The lower bound on  $\tan\beta$  affects the theoretically allowed regions in the  $(m_h, m_A)$  and  $(m_H, m_A)$  planes.

#### 4. Excluded mass regions at LEP1

In order to derive precise bounds on  $h^0$  and  $A^0$  masses, the limits on the Higgs boson production rates given in [12] have been used. In the mass plane  $(m_h, m_A)$ , each point with a step size of 1 GeV up to Higgs boson masses of 120 GeV has been analyzed separately. For each mass combination, the production cross sections of the reactions  $e^+e^- \rightarrow h^0 Z^{0*} \rightarrow h^0 \bar{f}f$ ,  $e^+e^- \rightarrow h^0 A^0$ , and the branching ratios for  $h^0$  and  $A^0$  decays have been computed as a function of the parameters described in Sec. 3<sup>3</sup>. Then, the number of expected Higgs boson events for each investigated final state and each mass bin has been calculated. The following channels are taken into account:

1.  $h^0$  production in bremsstrahlung processes:

$$e^+e^- \rightarrow h^0 Z^{0*} \rightarrow h^0 e^+e^-, h^0 \mu^+\mu^-, h^0 \bar{\nu}\nu$$

<sup>3</sup> The possibility of Higgs boson production via bremsstrahlung off b-quark  $e^+e^- \rightarrow b\bar{b} \rightarrow b\bar{b}h^0$  is not discussed. This channel could be significant for large values of  $\tan\beta$ . Also the fusion of  $W^+W^-$  is not considered as it is negligible for LEP1 and LEP2 energies. On the contrary, this reaction could become significant at the NLC [3].

2.  $h^0 A^0$  pair-production processes:

$$e^+e^- \rightarrow h^0 A^0 \rightarrow \tau^+\tau^-\tau^+\tau^-, \tau^+\tau^-\bar{b}b, \bar{b}b\bar{b}b.$$

For  $m_h > 2m_A$ :

$$e^+e^- \rightarrow h^0 A^0 \rightarrow A^0 A^0 A^0 \rightarrow \bar{b}b\bar{b}b\bar{b}b.$$

In addition, a combined LEP1 limit on non-standard  $Z^0$  decays has been applied:  $\Delta\Gamma_Z^{\max} < 31$  MeV at 95% CL [17]. A given  $(m_h, m_A)$  combination is excluded if for all SUSY parameter sets (from the ranges defined in Table I and for fixed  $m_t = 175$  GeV) the expected number of events in at least one of the channels is excluded at 95% CL.

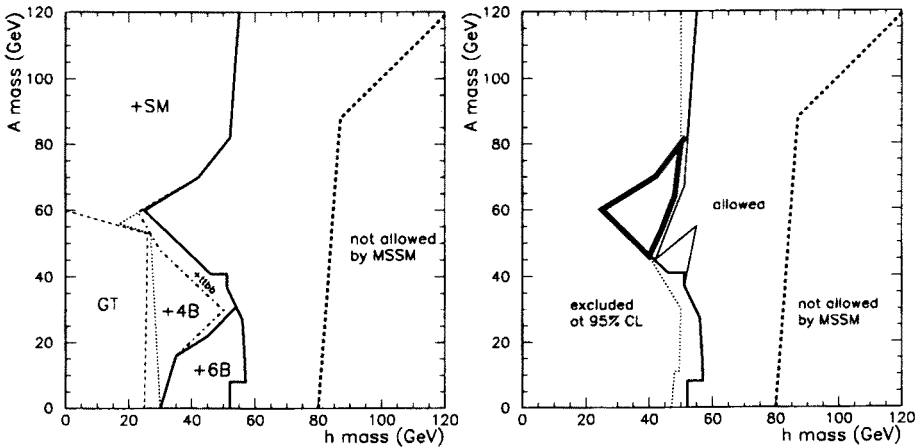


Fig. 1. Excluded mass regions at LEP1. Left plot — individually excluded mass regions for various searches (“GT”-  $Z^0$  lineshape; “SM”  $Z^0 \rightarrow Z^0 h^0$ ). Right plot — combined excluded regions: dotted line: EPA (epsilon approximation), thin solid line: FDC (heavy SUSY parameters only), thick solid line: FDC (scan over SUSY parameters), very thick line: new unexcluded region in FDC.

Left plot of Fig. 1 shows regions in the  $(m_h, m_A)$  plane which are excluded by the individual channels listed above. A comparison of the individual and combined excluded regions in left and right plots of Fig. 1 shows that the sum of the partial exclusion regions is smaller than the combined one. This is due to the scanning over the SUSY parameters. For fixed  $(m_h, m_A)$ , one can find the parameter combinations for which the cross section for a given channel is particularly low. It is unlikely that the cross sections are very low in all channels simultaneously, owing to the well-known complementarity of the cross sections of  $e^+e^- \rightarrow h^0 Z^0$  and  $e^+e^- \rightarrow h^0 A^0$  reactions. This complementarity holds approximately even after the inclusion of non-leading vertex corrections.

Right plot of Fig. 1 shows the regions in the  $(m_h, m_A)$  plane that can be excluded by the simultaneous analysis of all channels. Three regions are distinguished:

- (i) Excluded regions after performing a full scan over the SUSY parameter space and using the FDC method in cross section and branching ratio calculations;
- (ii) as above, but varying only  $m_{sq}$  and assuming that the other SUSY parameters are constrained to the values shown in Table II. This is done for comparison with the EPA approximation;
- (iii) excluded regions with radiative corrections calculated in the simplified EPA (“epsilon approximation”) [12], where only the leading corrections from the top and stop loops are taken into account. In this case results depend on  $m_{sq}$  only. The range  $175 \text{ GeV} \leq m_{sq} \leq 1000 \text{ GeV}$  is used.

TABLE II

Fixed heavy SUSY parameters used for comparison with the EPA results

Parameter	$m_{sq}$ (GeV)	$m_g$ (GeV)	$\mu$ (GeV)	$A$
Value	1000	1000	100	0

Right plot in Fig. 1 reveals an interesting result for the excluded regions in the  $(m_h, m_A)$  plane. The full scan over the SUSY parameter space (thick solid line) gives, in comparison with the epsilon approximation (dotted line, (iii)), a substantial additional triangle-shape unexcluded mass range for  $45 \text{ GeV} < m_A < 80 \text{ GeV}$  and  $25 \text{ GeV} < m_h < 50 \text{ GeV}$ , which is marked with a bold solid line. The existence of this region can be understood in the following way: in the range  $m_h + m_A < m_Z$  the reaction  $e^+e^- \rightarrow h^0 A^0$  is allowed kinematically and both main discovery channels  $e^+e^- \rightarrow h^0 Z^{0*}$ , and  $e^+e^- \rightarrow h^0 A^0$  contribute. If radiative corrections reduce the cross section of one of them below the experimental sensitivity, the complementary cross section will be large enough to exclude this mass combination. The unexcluded triangle begins just above the  $m_h + m_A = m_Z$  limit. In this range the bremsstrahlung cross section  $e^+e^- \rightarrow h^0 Z^{0*}$  can be small for some SUSY parameters. We identify points where it is suppressed by a factor of 25 compared with the MSM prediction for  $e^+e^- \rightarrow H_{\text{MSM}}^0 Z^{0*}$ . The complementary process is already forbidden kinematically, thus no signal can be observed. Low unexcluded  $m_h$  values are obtained for low physical stop masses of the order of  $\mathcal{O}(50 - 200 \text{ GeV})$  and large mixing in the sfermion sector ( $A = \pm 1$ , large  $\mu$ ), when the splitting between the left and right stop masses is large. The other SUSY parameters have smaller influence on the shape of the unexcluded region. With increasing  $m_A$ , the cross



section for the  $e^+e^- \rightarrow h^0 Z^{0*}$  reaction becomes less sensitive to the SUSY parameters and similar to the  $e^+e^- \rightarrow H_{\text{MSM}}^0 Z^{0*}$  cross section (calculated at  $m_h = m_{H_{\text{MSM}}^0}$ ) because of the decoupling effect [7]. The difference between cross sections calculated in the MSSM and MSM decreases as  $1/m_A^4$ . Above  $m_A \approx 100$  GeV the bremsstrahlung production of  $h^0$  is sufficient to establish, independent of the SUSY parameters, the Higgs mass bound of 55 GeV. Even in this range of  $m_A$ , for special SUSY parameter combinations (outside the values defined in Table I), a light  $h^0$  can escape detection for very large squark mixing.

Right plot in Fig. 1 shows that the regions obtained in approaches (ii) (thin solid line) and (iii) (dotted line) are similar. The excluded area in (ii) is only slightly larger than in (iii). The few GeV distance between the lines reflects the difference in the  $m_h$  values calculated in the EPA and the FDC. This shows that the EPA result can be approximately recovered for a specific set of SUSY parameters given in Table II.

The sizes of the excluded regions presented in Fig. 1 are rather insensitive to the choice of a lower bound on  $\tan\beta$ . The  $\tan\beta$  values from the range 0.5–1 are projected to  $m_h$  values ranging from 60 to 80 GeV, which is almost entirely above the reach of LEP1.

## 5. LEP2 discovery potential

Four production reactions relevant for LEP2  $e^+e^- \rightarrow h^0 Z^0, h^0 A^0$  and  $e^+e^- \rightarrow H^0 Z^0, H^0 A^0$  have been investigated based on sensitivities given in [13]. Each point in the  $(m_h, m_A)$  plane has been analyzed separately with a step size of 5 GeV. For each fixed mass combination (or fixed  $m_A$  and  $\tan\beta$ ), the production cross sections of all the four reactions have been calculated for  $\sqrt{s} = 175, 190$  and 210 GeV as a function of the parameters listed in the Sec. 2. When the first signal is visible,  $h^0$  and  $H^0$  are indistinguishable owing to low production rates and similar signatures. As a consequence, a given point in the parameter space is accessible at LEP2 if at least one of the cross sections  $\sigma_{hZ}, \sigma_{hA}, \sigma_{HZ}$  or  $\sigma_{HA}$  is larger than the expected experimental sensitivity. A linear interpolation has been used to obtain the sensitivity for mass combinations between simulated mass points. Four regions are distinguished in the  $(m_h, m_A)$  and  $(m_A, \tan\beta)$  planes:

- (A) The sensitivity region where, by direct searches, a Higgs signal cannot escape detection, for any choice of the SUSY parameters from the ranges given in Table I and for fixed top quark mass of 175 GeV.
- (B) The region where the perspectives of direct searches depend on the SUSY parameters. This means that searches can have sensitivity or not, depending on the specific choice of these parameters.

- (C) The non-sensitivity region where no signal can be found independent of the choice of the SUSY parameters.
- (D) The theoretically disallowed region in the  $(m_h, m_A)$  parameterization where  $(m_h, m_A)$  combinations are not allowed in the MSSM for any choice of SUSY parameters and requiring  $\tan \beta \geq 0.5$ .

The mass regions where at least one CP-even Higgs boson can be discovered at LEP2 for  $\sqrt{s} = 175, 190$  and  $210$  GeV are shown in the  $(m_h, m_A)$  and  $(m_A, \tan \beta)$  planes in Fig. 2.

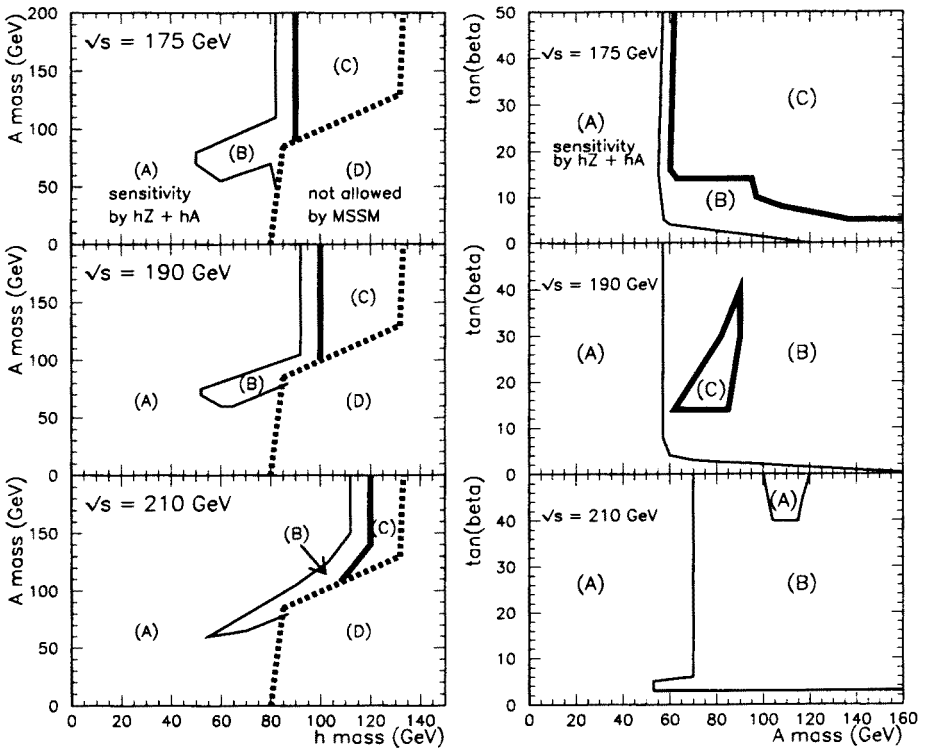


Fig. 2. Regions of detectability of  $h^0$  at LEP2 in the  $(m_h, m_A)$  (left plot) and  $(m_A, \tan \beta)$  (right plot) planes. For the description of regions (A)–(D) see text.

The effects of increasing center-of-mass energy can be clearly seen in the left plot of Fig. 2. A substantial region (B) reflects an uncertainty in the discovery potential connected with the variation over the SUSY parameters. The border between the regions (B) and (C) is largely set by the kinematical bound for the bremsstrahlung process  $e^+e^- \rightarrow h^0 Z^0$  and depends strongly on the available center-of-mass energy. The upper bound of region (C) depends mainly on the top quark mass. For  $m_A > 100$  GeV, region (B) forms

a band about 10 GeV wide, tangent to the kinematical bound. The second part of region (B) lies in the intermediate region  $m_h \approx m_A \leq 120$  GeV. For some combinations of the SUSY parameters even  $h^0$  as light as about 60 GeV can escape detection. Cross sections in this region are not much below the detection sensitivities and a fine-tuned experimental analysis can probably cover the low- $m_h$  part of region (B).

Right plot in the Fig. 2 shows the same results in the  $(m_A, \tan\beta)$  plane. The regions (A) are similar for  $\sqrt{s} = 175$  and 190 GeV. For  $\sqrt{s} = 210$  GeV the bound of region (A) shifts by about 15 GeV to about 70 GeV. For  $\sqrt{s} = 175$  GeV a large region (C) reflects the fact that there is no possibility to discover a MSSM scalar for  $m_A > 60$  GeV and  $\tan\beta > 5$ . Region (C) shrinks to small isolated area for  $\sqrt{s} = 190$  GeV and it is entirely replaced by region (B) for  $\sqrt{s} = 210$  GeV. This shows that for the higher center-of-mass energies the bremsstrahlung reaction  $e^+e^- \rightarrow h^0 Z^0$  can be observed even for large  $m_A$  values, with the exception of some choices of the SUSY parameters. For  $\sqrt{s} = 210$  GeV a small additional region (A) appears around the  $m_A = 100 - 120$  GeV and  $\tan\beta > 40$  due to  $H^0$  contributions.

Concluding, if the top quark mass is close to or higher than the central value of CDF measurements [16], even for  $\sqrt{s} = 210$  GeV and  $\mathcal{L} = 500 \text{ pb}^{-1}$  LEP2 cannot perform a decisive test of the MSSM. Most of the allowed  $(m_h, m_A)$  plane is covered, but some mass regions remain out of reach also for this machine configuration.

## 6. Discovery potential of the NLC

In the analysis of the physics potential of the NLC we use a center-of-mass energy of  $\sqrt{s} = 500$  GeV and an estimated sensitivity of 10 fb for all  $e^+e^- \rightarrow h^0 Z^0, H^0 Z^0, h^0 A^0$ , and  $H^0 A^0$  channels [3]. Assuming a total luminosity of the NLC of  $\mathcal{L} = 30 \text{ fb}^{-1}$ , this sensitivity corresponds approximately to a discovery of a signal if more than 300 events are produced (before selection cuts are applied). Under these assumptions the NLC can cover entirely the MSSM parameter space and at least one Higgs boson must be found or the MSSM is ruled out. This conclusion holds for a simultaneous search for the pair production reactions  $e^+e^- \rightarrow h^0 A^0, H^0 A^0$  and for the bremsstrahlung reactions  $e^+e^- \rightarrow h^0 Z^0, H^0 Z^0$ . The reaction  $e^+e^- \rightarrow h^0 Z^0$  alone is not sufficient because the cross section for this process is too low to be discovered for some parameter choices. At the NLC good chances exist to find more than one Higgs boson if its mass is not too large. Figure 3 (left plot) illustrates the perspectives of finding the heavier CP-even Higgs bosons  $H^0$ . Regions (A)–(D) are defined as in Sec. 4. Some fraction of the parameter space for  $m_A \leq 100$  GeV is covered by searches for  $H^0$  bremsstrahlung only. The remaining region can be covered by searches for  $H^0 A^0$  pair-production up to about  $m_A + m_H \leq 400$  GeV.

The discovery of more than one Higgs boson most clearly distinguishes the MSSM from the MSM. The important conclusion resulting from the analysis of the production rates of the neutral MSSM Higgs bosons at the NLC is that either  $h^0$  alone, or all three neutral MSSM scalars  $h^0$ ,  $H^0$  and  $A^0$  could be found simultaneously.

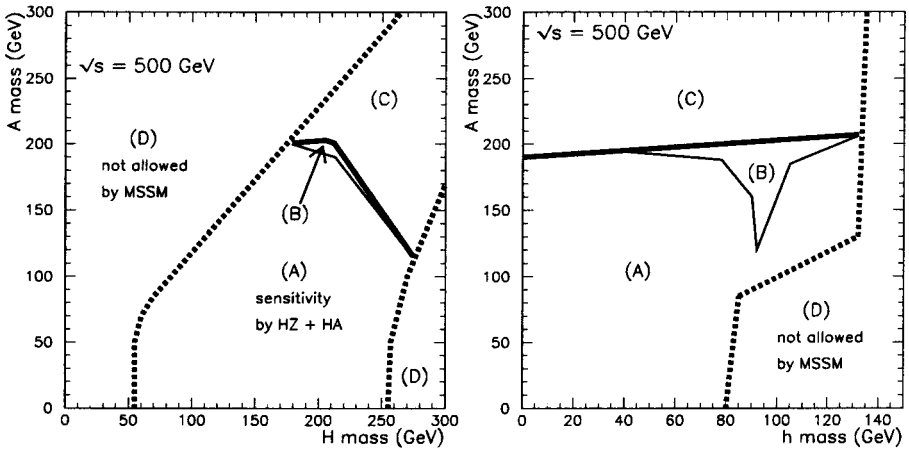


Fig. 3. Left plot: regions of detectability of  $H^0$  at the NLC. Right plot: regions of simultaneous detectability of  $h^0$ ,  $H^0$  and  $A^0$  at the NLC. For the description of regions (A)–(D) see text.

This is due to the complementarity of the couplings  $Z^0 Z^0 h^0$ ,  $Z^0 H^0 A^0$  and  $Z^0 Z^0 H^0$ ,  $Z^0 h^0 A^0$ . For  $m_A > 100$  GeV the cross section for the  $e^+e^- \rightarrow Z^0 h^0$  process and the  $h^0$  decay branching ratios are close to the MSM predictions [7]. In the same  $m_A$  range, the  $Z^0 H^0 A^0$  coupling is strong and  $Z^0 Z^0 H^0$  is weak, thus  $H^0$  can only be produced in association with  $A^0$  in the  $e^+e^- \rightarrow H^0 A^0$  reaction. For smaller  $A^0$  masses and some SUSY parameter choices,  $h^0$  bremsstrahlung cannot be observed. In this case the  $Z^0 Z^0 H^0$  and  $Z^0 h^0 A^0$  couplings are large and both process are kinematically allowed. Again all three neutral MSSM scalars could be detected. This conclusion also holds after taking into account the  $W^+W^-$  fusion:  $e^+e^- \rightarrow W^+W^- \nu \bar{\nu} \rightarrow \nu \bar{\nu} h^0(H^0)$ , since the  $W^+W^- h^0(H^0)$  and  $Z^0 Z^0 h^0(H^0)$  couplings are proportional. The right plot of Fig. 3, region (A), shows that all three scalars could be observed up to  $m_A \approx 200$  GeV. For  $m_h \approx 90$  GeV and  $m_A = 180$  GeV a small region (B) exists, where the perspectives of the simultaneous  $h^0$ ,  $H^0$  and  $A^0$  discovery depend on the SUSY parameters. For larger  $m_A$  only  $h^0$  can be found, region (C).

## 7. Conclusions

Aspects of searches for neutral supersymmetric Higgs bosons at present and future  $e^+e^-$  colliders have been presented. Full 1-loop diagrammatic calculations of radiative corrections to the Higgs particle production and decay rates are applied. The dependence of the results on all important model parameters is investigated. In addition to the stop mass, which is the most important free parameter in previous studies, several other SUSY parameters are varied independently. This variation changes significantly the results compared with the simpler EPA approach. We show that for fixed and heavy SUSY particle masses (and small left-right sfermion mass splitting) the results of the EPA can approximately be recovered in the FDC. Nevertheless, differences of the order of few GeV on the investigated Higgs mass bounds also exist in this case. Using detailed experimental results and performing a full scan over the MSSM parameters, the differences become large. For LEP1, FDC gives in comparison with EPA an additional unexcluded region for  $m_h \approx 25 - 50$  GeV and  $m_A \approx 45 - 80$  GeV.

For LEP2, the possibilities of a discovery of the lightest supersymmetric scalar depend strongly on the achievable center-of-mass energy. For  $m_A > 120$  GeV,  $h^0$  with the mass in the range  $m_h < (\sqrt{s} - 100)$  GeV could always be found. In the  $m_h$  range from  $(\sqrt{s} - 100)$  GeV up to the kinematical bound, perspectives of discovery depend on the specified set of the MSSM parameters.

At the NLC even at the most unfavourable parameter choice at least one MSSM neutral Higgs boson should be found or the MSSM is ruled out. The NLC has good chances to discover more than one Higgs particle, and most likely either one or all three MSSM neutral scalars could be observed.

## REFERENCES

- [1] ALEPH Collaboration, D. Buskulic *et al.*, *Phys. Lett.* **B313**, 312 (1993); DELPHI Collaboration, P. Abreu *et al.*, *Nucl. Phys.* **B373**, 3 (1992); L3 Collaboration, O. Adriani *et al.*, *Z. Phys.* **C57**, 355 (1993); OPAL Collaboration, R. Akers *et al.*, Preprint CERN, PPE/94-104 (1994).
- [2] Higgs Physics at LEP-II, M. Carena *et al.*, hep-ph/9602250, to be published in CERN yellow report, CERN-96-01.
- [3] Higgs Particles, A. Djouadi *et al.*, hep-ph/9605437, to appear in Proc. of the LC Workshop, DESY, Hamburg, April 1996.
- [4] J. Ellis, G. Ridolfi, F. Zwirner, *Phys. Lett.* **B257**, 83 (1991); H.E. Haber, R. Hempfling, *Phys. Rev. Lett.* **66**, 1815 (1991); Y. Okada, M. Yamaguchi, T. Yanagida, *Phys. Lett.* **B262**, 54 (1991); R. Barbieri, M. Frigeni, M. Caravaglios, *Phys. Lett.* **B258**, 167 (1991).

- [5] J. Ellis, G. Ridolfi, F. Zwirner, *Phys. Lett.* **B262**, 477 (1991); R. Barbieri, M. Frigeni, *Phys. Lett.* **B258**, 395 (1991); A. Brignole, J. Ellis, G. Ridolfi, F. Zwirner *Phys. Lett.* **B271**, 123 (1991).
- [6] M. Carena, K. Sasaki, C.E.M. Wagner, *Nucl. Phys.* **B381** 66; (1992); H.E. Haber, R. Hempfling, *Phys. Rev.* **D48**, 4280 (1993); M. Carena, M. Quiros, C.E.M. Wagner, *Nucl. Phys.* **B461**, 407 (1996).
- [7] P.H. Chankowski, S. Pokorski, J. Rosiek, *Phys. Lett.* **B281**, 100 (1992).
- [8] P.H. Chankowski, S. Pokorski, J. Rosiek, *Phys. Lett.* **B274**, 191 (1992); **B286**, 307 (1992); *Nucl. Phys.* **B423**, 437 (1994); **B423**, 497 (1994).
- [9] V. Driesen, W. Hollik, *Z. Phys.* **C68**, 485 (1995).
- [10] A. Brignole, *Phys. Lett.* **B281**, 284 (1992).
- [11] Z. Kunszt, F. Zwirner, *Nucl. Phys.* **B385**, 3 (1992).
- [12] L3 Collaboration, O. Adriani *et al.*, *Phys. Lett.* **B294**, 457 (1992); L3 Collaboration, O. Adriani *et al.*, *Z. Phys.* **C57** (1993), 355.
- [13] A. Sopczak, *Int. J. Mod. Phys.* **A9**, 1747 (1994).
- [14] J. Rosiek, *Phys. Rev.* **D41**, 3464 (1990); *erratum* hep-ph/9511250.
- [15] M. Böhm, W. Hollik, H. Spiesberger, *Fortschr. Phys.* **34**, 687 (1986); W. Hollik *Fort. Phys.* **38**, 165 (1990).
- [16] F. Abe *et al.*, CDF Collaboration, FERMILAB-PUB-94/097-E and FERMILAB-PUB-94/116-E.
- [17] A. Sopczak, *Mod. Phys. Lett.* **A10**, 1057 (1995).
- [18] *E.g.* B. Grzadkowski, J.F. Gunion *Phys. Lett.* **B243**, 301 (1990).